

# The Benzylphenylether Thermolysis Mechanism: Insights from Phase Behavior

The thermolysis of benzylphenylether (BPE) was examined at 320°C in liquid, vapor, and supercritical methanol phases as a probe of the reaction mechanism. Toluene and phenol were the major products in all cases, but observed selectivities were dependent upon the reaction phase. Isotopic labeling experiments demonstrated that methanol participated in the reaction network as a hydrogen donor through a free-radical mechanism. These results are consistent with free-radical steps for neat BPE primary pyrolysis that include BPE fission followed by hydrogen abstraction and radical recombination reactions. A detailed set of 21 free-radical steps quantitatively explains the dependence of the selectivity and conversion on the phase behavior.

**Benjamin C. Wu**

**Michael T. Klein**

**Stanley I. Sandler**

Center for Catalytic Science and Technology

Department of Chemical Engineering

University of Delaware

Newark, DE 19716

## Introduction

Supercritical fluid (SCF) solvents represent interesting and potentially powerful tools for reaction engineering because of their extreme P-V-T behavior near their critical point. As reaction media, SCF solvent properties can potentially be optimized via adjustments of pressure to improve reaction rates and selectivities. As we show here, SCF solvents can also be useful in the interpretation of kinetic information in the probe of reaction mechanisms.

Reported supercritical solvent effects include electrostatic interactions (Townsend et al., 1988; Johnston and Haynes, 1987), diffusional limitations (Lawson and Klein, 1985; Abraham, 1987; Helling and Tester, 1987; Yang and Eckert, 1988), and pressure effects (Johnston and Haynes, 1987; Simmons and Mason, 1972). However, the thermodynamic phase behavior can also affect global reaction kinetics and lead to interesting apparent solvent effects.

The reaction of dibenzylether (DBE) in supercritical toluene (Wu et al., 1989) provides an example of the influence of phase behavior on laboratory kinetics information. The conversion of DBE after 30 min at 375°C and constant initial DBE concentration,  $[DBE]_0$ , dropped from 90% at 5 atm to 50% at 48 atm, where the pressure increase was generated through the addition of toluene. Interpretation of the data by assuming a single-phase pressure effect would suggest an apparent activation volume of 2,000 cm<sup>3</sup>/mol, as much as three orders of magnitude greater

than typical intrinsic activation volumes (le Noble, 1978). However, phase equilibrium calculations showed the existence of a two-phase region that explained the drop in conversion without recourse to pressure-dependent rate constants.

Thus the adjustment of the pressure can also control the number and composition of phases in which a reaction occurs. This presents the opportunity to highlight the various elementary steps of a complex reaction mechanism since the concentrations of species can be varied easily by over two orders of magnitude by changing from the liquid to the vapor phase. This allows emphasis of, and discrimination between, unimolecular and bimolecular steps and their influence on global kinetics and selectivities. This is the object of the present paper, where we describe the reaction of BPE in liquid, vapor, and supercritical methanol phases.

## Background

The choices of both the supercritical solvent, methanol, and the substrate benzylphenylether (BPE: PhCH<sub>2</sub>OPh) were motivated by prior work. Because supercritical water hydrolyses a class of aromatic hydrocarbons (Townsend et al., 1988; Lawson and Klein, 1985; Helling and Tester, 1987; Yang and Eckert, 1988; Abraham and Klein, 1985; Abraham et al., 1988; Penninger, 1988a,b; Huppert et al., 1989), it seemed reasonable to anticipate the participation of supercritical methanol in solvolysis. While Abraham and Klein found that the reaction of benzylphenylamine (BPA: PhCH<sub>2</sub>NHPh) in supercritical methanol included the incorporation of a methoxy group in the products, the nature of the elementary steps—the involvement of polar molecules (Townsend et al., 1988; Huppert et al., 1989;

Correspondence concerning this paper should be addressed to M. T. Klein.

Townsend, 1989), ions (Penninger, 1988b; Antal et al., 1987; Ramayya et al., 1987), or free radicals—was not clear.

In this work, we studied similar mechanistic possibilities through reaction of the BPA analogue, BPE, whose thermal chemistry has been thoroughly studied (Schlosberg et al., 1981a,b, 1983; Virk, 1979; Frederick and Bell, 1984a,b; Mobley and Bell, 1979; Gilbert, 1984; King and Stock, 1982, 1984; Larsen and Lee, 1983; Takemura et al., 1981; Collins et al., 1977; Matsushashi et al., 1985; Korobkov et al., 1988a,b; Sato and Yamakawa, 1985; Stein, 1981) and therefore provided a convenient background to explore solvent effects.

The BPE thermolysis mechanism has also received considerable attention. The fission of the weak C–O bond is a consensus feature (Schlosberg et al., 1981b; King and Stock, 1984; Takemura et al., 1981; Matsushashi et al., 1985; Sato and Yamakawa, 1985), but subsequent steps remain equivocal because of their large number. Schlosberg (1981b) proposed a detailed set of reaction steps for the neat BPE pyrolysis in the liquid phase. Virk (1979) outlined an alternate pericyclic pathway for BPE pyrolysis in the presence of a hydrogen donor such as tetralin or decalin. In this work, reactions in the gas and liquid phase and in supercritical methanol allowed sequential emphasis of unimolecular, bimolecular, and BPE fission elementary steps, respectively.

The present work was therefore aimed at both resolving the role of supercritical methanol in reaction chemistry and using phase behavior to extend previous studies of the BPE pyrolysis mechanism. The experimental methods and results are presented first. The discussion that then follows describes a rather detailed mechanism that is nevertheless susceptible to both complete numerical and simplified analysis.

## Experimental Methods

BPE was pyrolyzed in 316 stainless steel “tubing bomb” reactors with volumes of 0.59 and 5 cm<sup>3</sup>. A summary of the conditions is shown in Table 1. The reactors consisted of a Swagelok port connector and two end caps; the fittings were 1/4 in. for the 0.59 cm<sup>3</sup> reactors and 1/2 in. for the 5 cm<sup>3</sup> version. BPE, biphenyl (BP), a demonstrably inert (Townsend and Klein, 1985) internal standard, and methanol ( $\rho_r = 1.2$ ), whenever necessary, were loaded volumetrically into the tubing bombs with an Eppendorf digital pipette ( $\pm 1\%$ ); the loadings were verified with a Mettler AE200 balance ( $\pm 0.1$  mg). The

**Table 1. Experimental Conditions\* and Results**

Loadings mol/L <sub>R</sub>	Liquid Phase	Vapor Phase	SC Methanol
BPE	0.185	0.054	0.046
BP	0.220	0.065	0.056
Methanol	none	none	10.17
Conversion, x	0.90	0.42	0.20
Average Selectivities			
Toluene	0.35	0.15	0.57
Phenol	0.49	0.61	0.56
Benzaldehyde	0.04	0.2	<0.01
OHD	0.09	0.04	<0.01
Products Identified, %			
91			95

\*All experiments performed at 320°C up to a final time of 20 minutes. Diphenyl ketone and benzene were also detected in trace amounts (<1% yield).

reactors were heated to, and maintained at, a reaction temperature of  $320 \pm 2^\circ\text{C}$  in a fluidized sand bath. After the final reaction time was reached, the reactions were quenched by immersing the tubing bombs in a room-temperature ( $\sim 20^\circ\text{C}$ ) water bath. The reaction products were recovered by three consecutive acetone washes. The products were then identified by GC/MS and quantified on an HP 5580 GC equipped with a 50 m DB-5 fused silica capillary column and flame ionization detector. Response factors were determined by analyzing standard mixtures.

Isotopic labeling experiments were performed using fully deuterated methanol (CD<sub>3</sub>OD). The extent of deuterium incorporation into toluene was determined using a Hewlett-Packard 5890/5970 gas chromatograph/mass spectrometer. Phenol isotopes were not examined because they are prone to undesired isotopic exchanges during analysis (Brodschii, 1943).

## Calculation of Phase Behavior

The phase behavior of the reaction mixtures was controlled through the reactant loadings and calculated using a modified flash program. The detailed calculations are reported elsewhere (Wu et al., 1989). The Peng-Robinson equation of state was used to describe the nonidealities because of its correlative accuracy in methanol–coal model compound systems (Thies, 1985), albeit without interaction parameters. Therefore, experimental loadings were well beyond phase boundaries to assure essentially one-phase reaction.

For neat BPE reactions, a dew point BPE loading,  $[BPE]_{dp}$ , was calculated as 0.074 mol/L<sub>R</sub>; loadings above  $[BPE]_{dp}$  induced the formation of a liquid phase. Therefore, a loading of 0.054 mol/L<sub>R</sub> was used for vapor phase pyrolysis, which is  $\sim 25\%$  less than  $[BPE]_{dp}$ . The nominal liquid-phase BPE loading of 0.46 mol/L<sub>R</sub> caused essentially all (>99.9%) of the BPE to be present in the liquid.

The BPE/supercritical methanol phase behavior at 320°C is presented in Figure 1. The experimental conditions used for the reaction of BPE in methanol were significantly removed from those for the calculated two-phase regions. The results from these experiments were therefore interpreted as being from single-phase experiments.

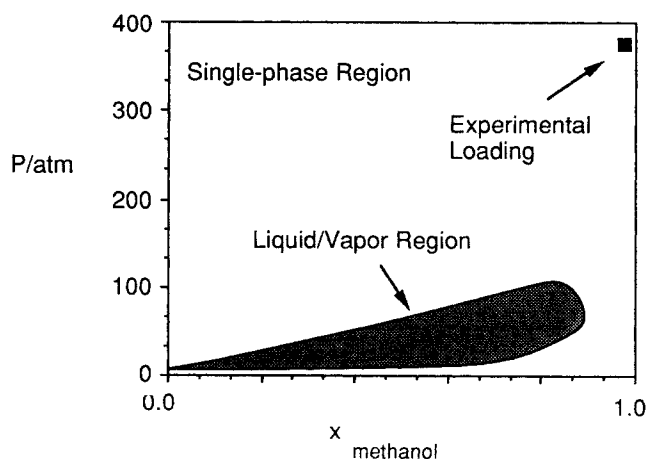


**Figure 1. Phase behavior of BPE/methanol systems at 320°C.**

## Results

Representative results are shown in Table 1. Toluene and phenol were the major products from BPE pyrolysis in the liquid, vapor, and supercritical methanol phases. In addition, benzaldehyde was produced from vapor-phase BPE pyrolysis.

The temporal variations of the BPE, toluene, and phenol yield ( $y_i = N_i/N_{\text{BPE}0}$ ) are presented in Figures 2, 3, and 4. The conversion of BPE,  $x = 1 - y_{\text{BPE}}$ , at 20 min was approximately 0.9 in the liquid phase, 0.6 in the vapor phase, and 0.2 in supercritical methanol.

The dependence of the product selectivities on the fluid phase is emphasized in Figure 5, a plot of the major product yields vs. conversion. The slopes of linear least-square fits provide average product selectivities, which, for toluene, varied dramatically from  $0.15 \pm 0.05$  in the vapor phase, to  $0.35 \pm 0.02$  in the liquid phase, and  $0.57 \pm 0.03$  in supercritical methanol. The dependence of the phenol selectivity on the reaction phase was less pronounced:  $0.61 \pm 0.14$  in the vapor phase,  $0.49 \pm 0.02$  in the liquid phase, and  $0.57 \pm 0.03$  in supercritical methanol. The toluene and phenol selectivities in supercritical methanol were more similar to those in the liquid than in the vapor phase, although the conversion was more similar to that in the vapor phase.

The foregoing shows that reaction of BPE in supercritical methanol led to equimolar formation of toluene and phenol. This is similar to previous reactions in tetralin (Collins, 1977; Korobkov et al., 1988a,b; Sato and Yamakawa, 1985), which suggests that methanol was a hydrogen donor. This motivated the reaction of BPE in fully deuterated ( $\text{CD}_3\text{OD}$ ) supercritical methanol. Approximately 55% of the toluene produced was singly deuterated ( $\text{PhCH}_2\text{D}$ ), the remainder being fully protonated ( $\text{PhCH}_3$ ). This suggests that the free-radical hydrogen transfer from BPE was about 170 times faster than from methanol; see Table 1 for relative concentrations. Note that heterolytic reaction involving methanol would have led to different products and isotopic exchange.

## Discussion

The observed dependence of BPE conversion and average product selectivities on the phase behavior provides information about the kinetics of the elementary steps of pyrolysis. The

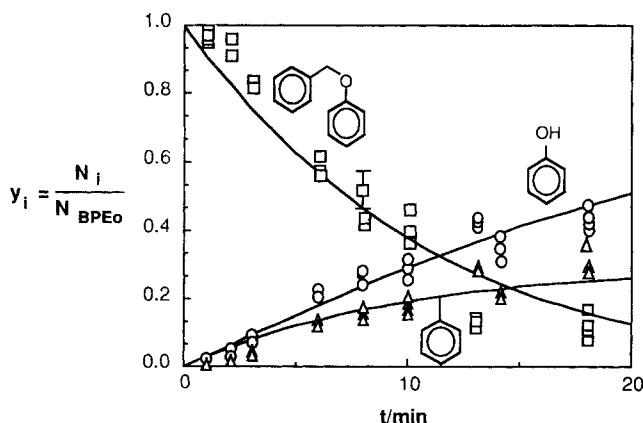


**Figure 2. Temporal variation of product yields from BPE pyrolysis in liquid phase at 320°C.**

△ toluene; ○ phenol; □ BPE

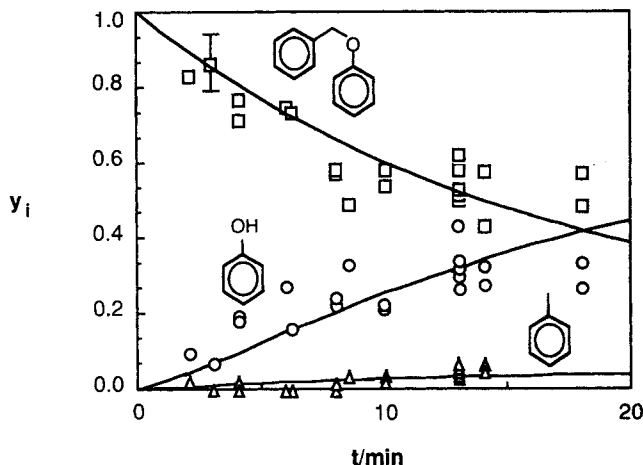


**Figure 3. Temporal variation of product yields from BPE pyrolysis in vapor phase at 320°C.**

△ toluene; ○ phenol; □ BPE

discussion to follow is aimed at extending and solving a set of steps for BPE pyrolysis and its reaction in supercritical methanol. The model is based on and therefore provides insights into the observed dependence of the reaction kinetics and selectivity on the phase behavior.

### Elementary steps for BPE pyrolysis

The elementary steps of BPE pyrolysis can be organized into primary and secondary groups. The primary steps involve BPE and are presented in Figure 6. These are similar to those proposed by Schlosberg et al. (1981b) for BPE and analogous to those proposed by Stein (1981) for the pyrolysis of diphenylethane. The initial step is the fission of the weak C–O bond to form benzyl ( $\gamma_1$ ) and phenoxy ( $\gamma_2$ ) radicals. These can in turn abstract hydrogen from BPE, forming the two major products, toluene and phenol, and a BPE radical ( $\mu_1$ ). The recombination steps involve all the possible combinations of radical species. None of the primary termination products formed in measurable quantities. However, Schlosberg et al. (1981b) detected the

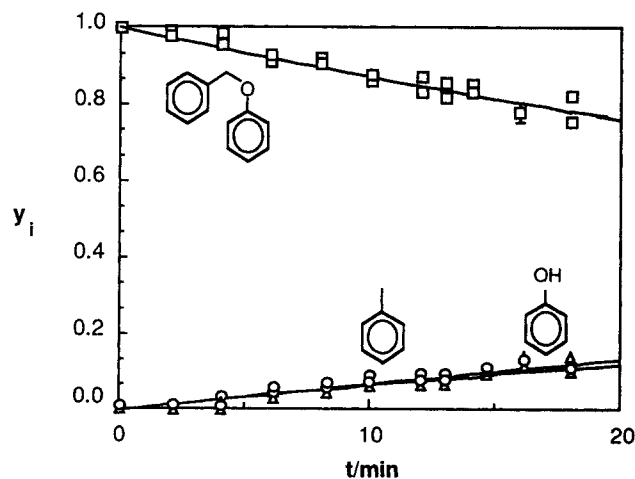


**Figure 4. Temporal variation of product yields from pyrolysis in SC methanol ( $p_r = 1.2$ ) at 320°C.**

△ toluene; ○ phenol; □ BPE

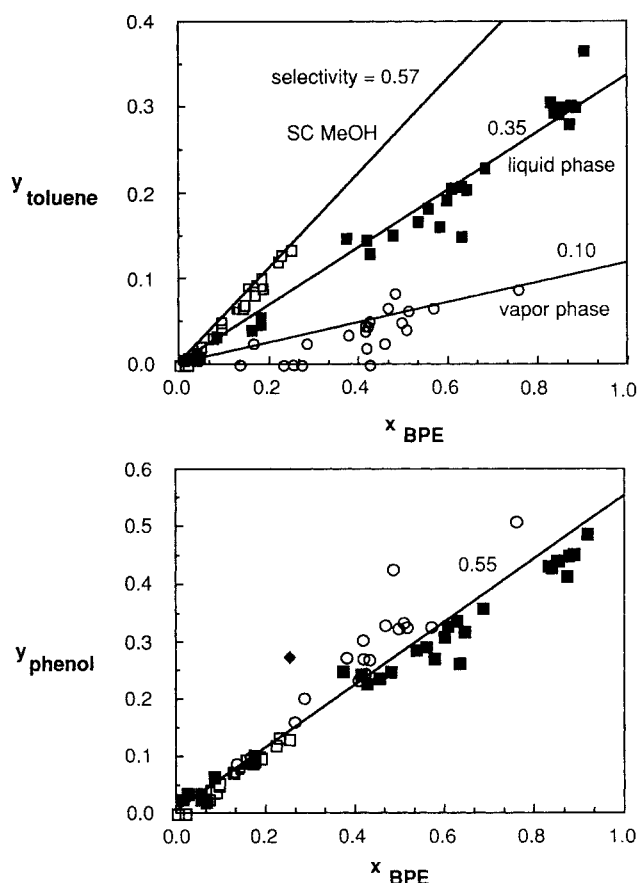


**Figure 5. Effect of fluid phase on toluene and phenol selectivity from BPE pyrolysis at 320°C.**

□ supercritical methanol; ■ liquid; ○ vapor

two most stable termination products, bibenzyl and phenoxydiphenylethane, from their experiments in the liquid phase.

The primary termination products can undergo secondary reactions, as shown in Figure 7. The secondary reactions play three roles. First, the primary termination products (TP) can generate  $\gamma_2$  (phenoxy) radicals from bond fission or lead to  $\gamma_2$  from  $\beta$  scission of the radicals formed from the hydrogen abstraction of TP. Second, TP can provide hydrogen to cap radical species. Finally, the secondary reactions generate olefinic materials that are particularly prone to polymerization reactions, eventually forming char. The net effect of the termination of the primary radicals is the subsequent generation of  $\gamma_2$  radicals and char; the formation of  $\gamma_1$  radicals from TP is negligible. This explains why the selectivity to phenol was always greater than or equal to that for toluene, Figure 4.

BPE pyrolysis in methanol involves at least two additional steps, such as those shown in Figure 8. The labeling results suggesting hydrogen abstraction from BPE to be approximately 170 times faster than hydrogen abstraction from methanol are consistent with thermochemical estimates. An Evans-Polanyi  $\alpha \sim 0.25$  and C-H bond strengths of  $\sim 70.5 \pm 2 \text{ kcal} \cdot \text{mol}^{-1}$  ( $\sim 295.4 \pm 8.4 \text{ kJ} \cdot \text{mol}^{-1}$ ) and  $94 \pm 2 \text{ kcal} \cdot \text{mol}^{-1}$  ( $394 \pm 8.4 \text{ kJ} \cdot \text{mol}^{-1}$ ) for BPE and methanol (McMillen and Golden, 1982), respectively, indicate that H transfer from BPE would be 60 to 330 times faster than from methanol.

The ostensibly formidable number of steps in Figures 6–8 is

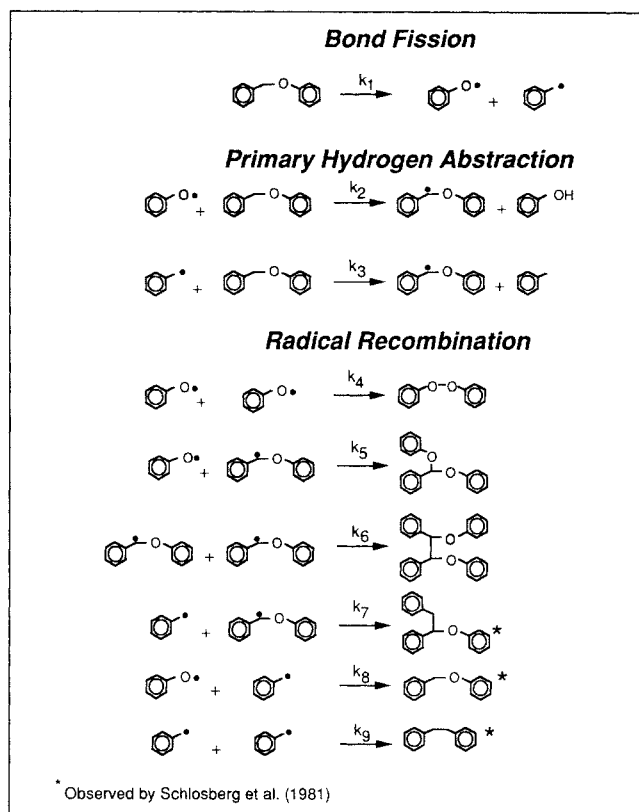


**Figure 6. Elementary steps for primary BPE pyrolysis.**

actually quite reasonable. BPE has only two weak bonds: the central C-O bond is one and the benzylic C-H bond is the other. All other bond strengths are of the order of 20–30 kcal/mol (84–126 kJ/mol) stronger and therefore are uninvolved in the major pyrolysis chemistry at 320°C. Rate constants involving these strong bonds would be about 7–11 orders of magnitude smaller than those for the weak bonds at 320°C.

Thus, the mechanism is quite straightforward. The weakest (C-O) bond ruptures to give two free radicals (step 1), which can recombine or abstract hydrogen from BPE. The latter steps generate the products and a third radical. The termination steps, 4–9, represent the seven allowable combinations of three different species minus the one leading to highly unstable peroxides.

The secondary reactions are likewise in accord with basic thermochemical kinetics (Stein, 1981; McMillan and Golden, 1982).

Solution of the kinetics model of Figures 6–8 provides a prediction of yield and selectivity and, with quantitative comparison to Figures 2–4, a measure of the model likelihood,  $Q(X^2/v)$  (Press et al., 1986). This requires numerical values for the 21 rate constants of Figures 6–8. At one extreme, estimation of all 21 parameters through the fit of the model to the experimental data would provide a low model likelihood ( $Q \ll 1$ ) because of the low degrees of freedom,  $v = n - m$ , where  $n$  is the number of experimental data points and  $m$  is the number of regressed parameters. At the other extreme, *a priori* prediction of each  $k$  would result in low model likelihood because of the anticipated large deviation of the model predictions from the data. An optimal resolution was to lump by reaction families, in which

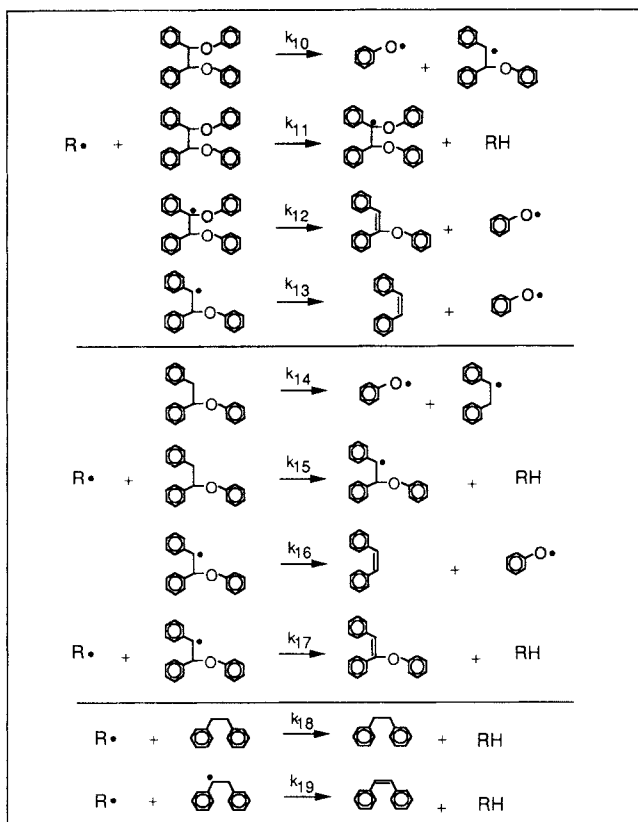


Figure 7. Elementary steps for secondary BPE pyrolysis.

each family member (reaction) had an identical  $k$ , and use a mix of *a priori* predictions and optimized constants.

Following this logic, the rate constants for  $\beta$  scission and disproportionation reaction families were derived from literature activation parameters (Stein, 1981) as  $10^{10} \text{ s}^{-1}$  and  $553 \text{ s}^{-1} \cdot \text{M}^{-1}$ , respectively, for  $T = 320^\circ\text{C}$ . The rate constants for the fission, hydrogen abstraction, and radical recombination reaction families ( $k_f$ ,  $k_H$ , and  $k_T$ ) were optimized using the downhill simplex method of Nelder and Mead (1965) and the  $\chi^2$  minimization function of Eq. 1.

$$\chi^2 = \sum_{i=1}^n (y_{\text{exp},i} - y_{\text{model},i})^2 / \sigma_i^2 \quad (1)$$

where  $n$  is the number of experimental observations,  $y$  the model prediction or experimental measurement, and  $\sigma_i$  the standard deviation of the measurement. The values of  $k_f$ ,  $k_H$ , and  $k_T$  were anticipated to be different for each phase (Stein et al., 1982).

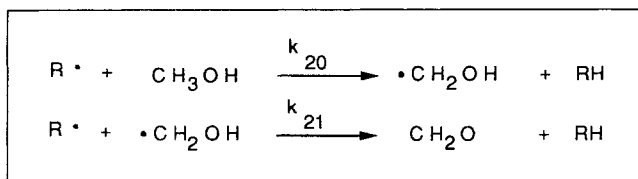


Figure 8. Hydrogen donation mechanism for BPE pyrolysis in SC methanol.

However, we emphasize that three and not 21 rate coefficients were determined via model optimization to the kinetics data.

Optimized values of  $k_f$ ,  $k_H$ , and  $k_T$  are listed in Table 2. They fall essentially within an order of magnitude of *a priori* estimates (Stein, 1981). The confidence limits of the rate constants were calculated using a standard Monte Carlo method (Press et al., 1986; Landau et al., 1988).

These optimized rate constants provide the correlation of the experimental data represented as solid lines in Figures 2, 3, and 4. The error bars represent the 95% confidence limit on the accuracy of the experimental data. Model likelihood parameters are listed in Table 3. The model provides as excellent correlation for BPE pyrolysis in supercritical methanol and a reasonable depiction of liquid- and vapor-phase pyrolysis.

This detailed model allows emphasis of the differences between the liquid- and vapor-phase BPE pyrolysis. In addition to the predictions of the experimental observables, unobservables such as radical concentrations or instantaneous rates can be computed. For example, the temporal variations of the yields of the three most abundant reactive intermediates,  $\gamma_1$ ,  $\gamma_2$ , and  $\mu_1$ , are plotted in Figures 9 and 10 for reaction in the liquid and the vapor phase, respectively, along with the relative yield of phenol to toluene. Two differences are particularly striking. First,  $\mu_1$  is the most abundant reactive intermediate in the liquid phase and the least abundant of these three intermediates in the vapor phase. Second, the ratio  $\gamma_2/\gamma_1$  is significantly larger in the vapor phase than in the liquid phase. The first observation indicates the relative importance of the hydrogen abstraction steps in the liquid phase. The second observation implies that the secondary reactions are more prevalent in the vapor than the liquid phase since  $\gamma_2$ , not  $\gamma_1$ , is generated in secondary reactions.

These radical concentrations control the experimental observations and their sensitivity in the reaction phase. In the absence of secondary reactions,  $\gamma_1$  and  $\gamma_2$  are identical, as are  $y_{\text{phenol}}$  and  $y_{\text{toluene}}$ . The secondary reactions are manifested experimentally as higher yields of phenol to toluene, that is,  $y_{\text{phenol}}/y_{\text{toluene}} > 1$ . In the liquid-phase BPE pyrolysis, Figure 9,  $y_{\text{phenol}}/y_{\text{toluene}}$  approaches unity near zero conversion, where secondary reactions are essentially negligible. However, the secondary reaction steps are never negligible experimentally in the vapor phase, because of the rapidity of the termination steps, and  $y_{\text{phenol}}/y_{\text{toluene}}$  does not approach unity at any measurably low conversion.

Another measure of the importance of secondary reactions is the ratio,  $r_p/r_{T_s}$ , of the primary hydrogen abstraction rate (steps 2–3) to the primary termination rate, since the latter reaction forms products susceptible to secondary reaction. The dependence of  $r_p/r_{T_s}$  on the reaction phase is shown in Figure 11 as a

Table 2. Optimized Rate Constants for BPE Pyrolysis Reaction Families at  $T = 320^\circ\text{C}$

Reaction Family	Reaction Phase		
	SC Methanol	Liquid	Vapor
Bond fission, $k_f \times 10^4 \text{ s}^{-1}$	$1.3 \pm 0.1$	$5.7 \pm 0.3$	$23.8 \pm 21.3$
H-abstraction, $k_H \times 10^{-2} \text{ s}^{-1} \cdot \text{M}^{-1}$	$111.7 \pm 115.0$	$85.2 \pm 83.0$	$1.1 \pm 2.2$
Termination, $k_T \times 10^{-3} \text{ s}^{-1} \cdot \text{M}^{-1}$	$0.32 \pm 0.96$	$10.56 \pm 12.2$	$0.10 \pm 0.06$

**Table 3. Statistical Likelihood of BPE Thermolysis Reaction Models**

Phase	<i>n</i>	<i>m</i>	$\sigma_{ave}$	$\chi^2$	<i>Q</i>
Liquid	30	3	0.02	160.8	$3.1 \times 10^{-6}$
Vapor	20	3	0.03	111.2	$2.5 \times 10^{-5}$
SC Methanol	22	3	0.01	69.2	0.3

plot of  $r_{Pr}/r_{Te}$  vs. conversion, parametric in  $[BPE]_0$ . Since hydrogen abstraction generates both toluene and phenol and secondary reactions only the latter, increases in  $r_{Pr}/r_{Te}$  direct  $y_{phenol}/y_{toluene}$  toward unity, which was observed experimentally.

### Simplified analysis

This discussion points to the ratio  $r_{Pr}/r_{Te}$  as an indicator of the relative yields of phenol and toluene. This issue can be probed through a simple steady-state analysis that balances the generation of radicals from BPE with their termination, that is,

$$k_I [BPE] = k_T [R\cdot]^2 \quad (2)$$

where

$$[R\cdot] = \mu_1 + \gamma_1 + \gamma_2 \quad (3)$$

The balance of Eq. 2 is most appropriate at low conversions where BPE is the only significant radical source. Under these conditions, the rate of hydrogen abstraction will provide the rate

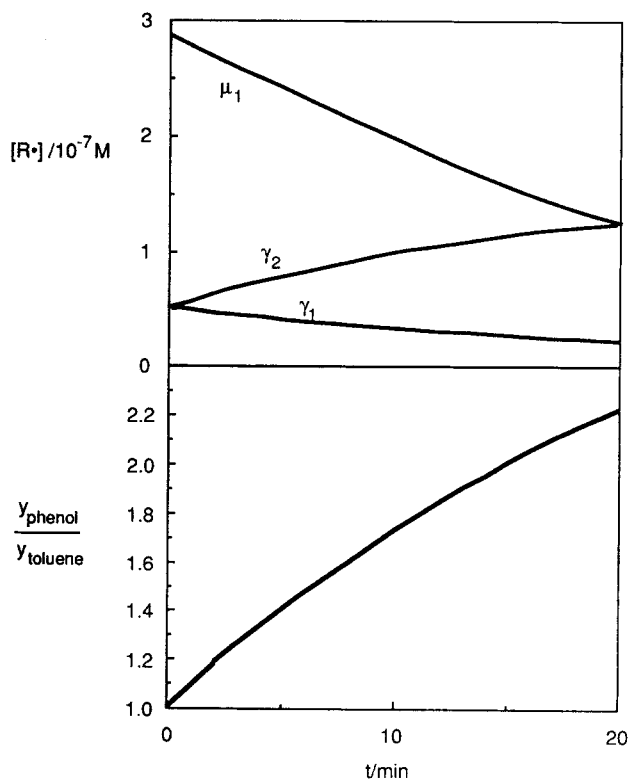


**Figure 9. Model prediction of liquid-phase temporal variation of radical concentrations and major product yield ratio.**

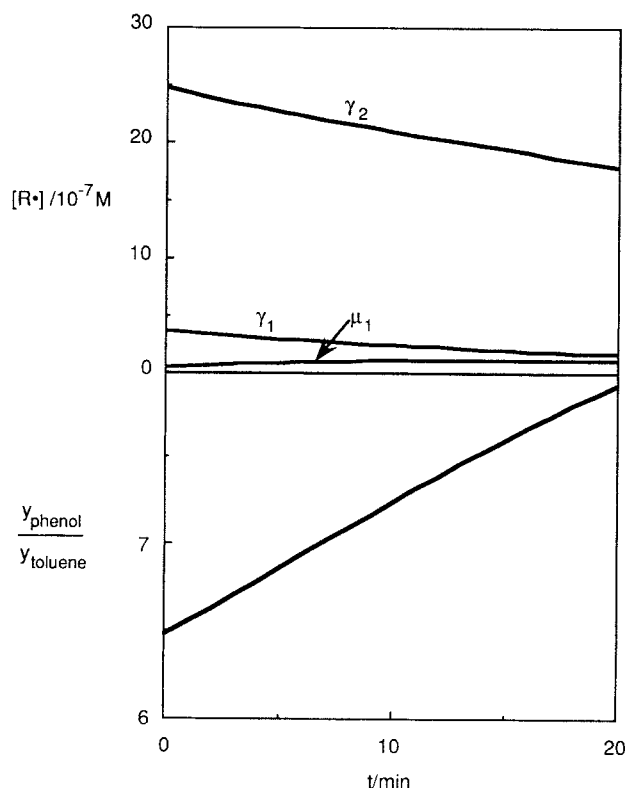


**Figure 10. Model prediction of vapor-phase temporal variation of radical concentrations and major product yield rates.**

of generation of toluene and the rate of generation of phenol from primary steps as:

$$r_{Pr} = k_H [R\cdot] [BPE] = k_H \sqrt{\frac{k_I}{k_T}} [BPE]^{3/2} \quad (4)$$

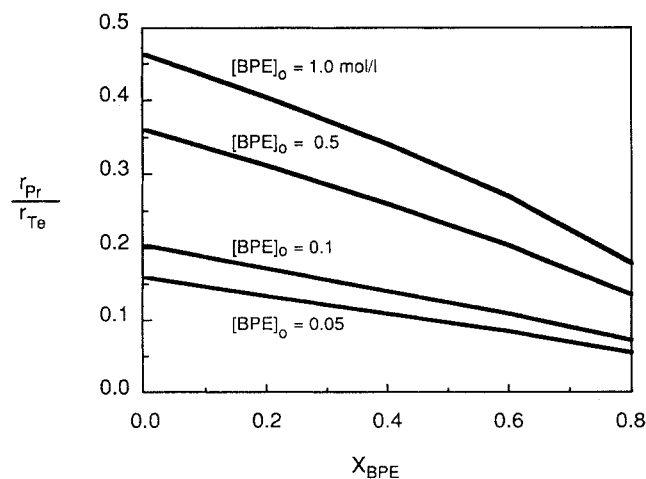


**Figure 11. Effect of concentration and conversion on relative rates of primary hydrogen abstraction and termination.**

Equation 2 provides the termination rate as

$$r_{Te} = k_t [BPE] \quad (5)$$

This is the indicator of the importance of secondary reactions, which produce phenol, not toluene. Equations 2 and 3–5 combine to provide an indicator,  $I$ , of the relative rates of formation of phenol and toluene as

$$I = \frac{r_{P_r} + r_{T_r}}{r_{P_r}} = 1 + \frac{k'}{[BPE]^{1/2}} \quad (6)$$

Equation 6 shows  $I$  (phenol to toluene index) to decrease with increases in  $[BPE]$ , as was observed. For reactions in methanol the source of radicals is unchanged. Therefore Eq. 2 is still valid with the provision that  $R\cdot$  include methoxy radicals, which disproportionate according to Figure 8. The primary rate of formation of toluene and phenol will include a term for the hydrogen transfer from methanol as

$$\begin{aligned} r_{P_r} &= k_H [R\cdot] [BPE] + k'_H [R\cdot] [MeOH] \\ &= k'' [BPE]^{3/2} + k''' [BPE]^{1/2} [MeOH] \quad (7) \end{aligned}$$

In this instance the indicator  $I$  of the relative rates of formation of phenol and toluene reduces as

$$I = \frac{k'' [BPE]^{3/2} + k''' [BPE]^{1/2} [MeOH] + k_t [BPE]}{k'' [BPE]^{3/2} + k''' [BPE]^{1/2} [MeOH]} \quad (8)$$

which approaches unity as  $[MeOH]$  approaches a large value. This was observed experimentally.

In summary, the primary reaction steps produce essentially equal moles of phenol and toluene and the secondary steps produce phenol and char. The production of phenol is therefore always equal to or greater than that of toluene. In supercritical methanol, methanol acts as a free-radical hydrogen source, which promotes an equimolar production of phenol and toluene.

## Conclusions

The pyrolysis of BPE in different fluid phases provided valuable insight into the reaction mechanism. The product selectivities and conversions varied significantly in the liquid, vapor, and supercritical methanol phases. A mechanism for BPE pyrolysis has been suggested that involves both primary free-radical reactions of the substrate and secondary radical steps for each of the primary termination products. The dependence of the selectivities and conversion on the phase behavior were attributed mostly to the variations of the concentration of BPE and its effect on primary vs. secondary reaction steps. Finally, methanol participated as a hydrogen donor by a free-radical mechanism.

## Notation

BP = biphenyl (PhPh)  
BPA = benzylphenylamine (PhCH<sub>2</sub>NHPh)  
BPE = benzylphenylether (PhCH<sub>2</sub>OPh)  
 $k$  = rate constant  
 $m$  = number of adjustable parameters  
 $n$  = number of experimental data points  
 $P$  = pressure, atm

$TP$  = termination product  
 $Q$  = model likelihood  
 $R\cdot$  = sum of radical concentrations  
 $S$  = selectivity  
 $T$  = temperature, K  
 $x$  = conversion,  $1 - y_{BPE}$   
 $y$  = yield,  $[N_i]/[N_{BPE}]_0$

## Greek letters

$\alpha$  = Evans-Polanyi constant  
 $\delta$  = solubility parameter  
 $\epsilon$  = dielectric constant  
 $\gamma_1$  = benzyl radical  
 $\gamma_2$  = phenoxy radical  
 $\mu_1$  = BPE radical  
 $\eta$  = viscosity  
 $\rho$  = density  
 $\sigma_i$  = standard deviation of measurement  $i$   
 $v$  = degrees of freedom =  $n - m$   
 $\chi^2$  = chi squared

## Subscripts

$c$  = critical property  
 $dp$  = dew point  
 $i$  = component  $i$   
 $I$  = initiation (bond fission)  
 $liq$  = liquid phase  
 $o$  = initial condition  
 $P_r$  = primary hydrogen abstraction reaction  
 $r$  = reduced property,  $A/A_c$   
 $R$  = reactor  
 $S$  = secondary reaction  
 $T_e$  = termination step (radical recombination or disproportionation)  
 $vap$  = vapor phase

## Literature Cited

- Abraham, M. A., "Reactions with Supercritical Fluid Solvents of Heteroatom-containing Model Compounds of Heavy Feedstocks," PhD Thesis, Univ. Delaware (1987).  
Abraham, M. A., and M. T. Klein, "Pyrolysis of Benzylphenylamine Neat and with Tetralin, Methanol, and Water Solvents," *Ind. Eng. Chem. Prod. Res. Dev.*, **24**, 300 (1985).  
Abraham, M. A., B. C. Wu, S. C. Paspek, and M. T. Klein, "Reactions of Dibenzylamine Neat and in Supercritical Solvents," *Fuel Sci. Technol. Int.*, **5**, 557 (1988).  
Antal, M. J., Jr., A. Brittain, C. DeAlmeida, S. Ramayya, and C. R. Jiben, "Heterolysis and Homolysis in Supercritical Water," *ACS Symp. Ser.*, **329**, 77 (1987).  
Brodskii, A. I., *Izvest. Akad. Nauk S.S.S.R., Otdel. Khim. Nauk.*, (1943).  
Collins, C. J., V. F. Raaen, B. M. Benjamin, and G. W. Kabalka, "Carbon-Carbon Cleavage During Asphaltene Formation," *Fuel*, **56**, 107 (1977).  
Frederick, T. J., and A. T. Bell, "Cleavage of Benzylaryl Ethers in the Presence of Zinc Halides," *J. Catal.*, **87**, 210 (1984a).  
———, "Cleavage of Dibenzyl Ether in the Presence of Zinc Halides," *J. Catal.*, **87**, 226 (1984b).  
Gilbert, K. E., "Coal Liquefaction Model Studies: Radical-Initiated and Phenol-Inhibited Decomposition of 1,3-Diphenylpropane, Dibenzyl Ether, and Phenethyl Phenyl Ether," *J. Org. Chem.*, **49**, 6 (1984).  
Helling, R. H., and J. W. Tester, "Oxidation Kinetics of Carbon Monoxide in Supercritical Water," *Energy and Fuels*, **1**, 417 (1987).  
Huppert, G. L., B. C. Wu, S. H. Townsend, M. T. Klein, and S. C. Paspek, "Hydrolysis in Supercritical Water: Identification and Implications of a Polar Transition State," *Ins. Eng. Chem. Res.*, **28**, 161 (1989).  
Johnston, K. P., and C. Haynes, "Extreme Solvent Effects on Reaction Rate Constants at Supercritical Fluid Conditions," *AIChE J.*, **33**, 2017 (1987).  
King, H., and L. M. Stock, "Aspects of the Chemistry of Donor Solvent Coal Dissolution. The Role of Phenol in the Reaction," *Fuel*, **61**, 1172 (1982).

- , "Aspects of the Chemistry of Donor Solvent Coal Dissolution," *Fuel*, **63**, 810 (1984).
- Korobkov, V. Y., E. N. Grigorieva, V. I. Bykov, O. V. Senko, and I. V. Kalechitz, "Effect of the Structure of Coal-Related Model Ethers on the Rate and Mechanism of Their Thermolysis. 1: Effect of the Number of Methylene Groups in the  $R-(CH_2)_n-O-(CH_2)_m-R$  Structure," *Fuel*, **67**, 657 (1988a).
- , "Effect of the Structure of Coal-Related Model Ethers on the Rate and Mechanism of Their Thermolysis. 2: Effect of Substituents in the  $C_6H_5-CH_2-O-C_6H_4-X$  Structure," *Fuel*, **67**, 663 (1988b).
- Landau, R. N., C. Libanati, and M. T. Klein, "Monte Carlo Simulation of Lignin Pyrolysis: Sensitivity to Kinetic Parameters," *Research in Thermochemical Biomass Conversion*, A. V. Bridgewater, and J. L. Kuester, eds., Elsevier, New York (1988).
- Larsen, J. W., and D. Lee, "Reactions of Coal in Acidic Phenol. Model Compound Studies," *Fuel*, **62**, 463 (1983).
- Lawson, J. R., and M. T. Klein, "Influence of Water on Guaiacol Pyrolysis," *Ind. Eng. Chem. Res.*, **24**, 203 (1985).
- le Noble, W. J., "Activation and Reaction Volumes in Solution," *Chem. Rev.*, **78**(4), 409 (1978).
- Matsushashi, H., H. Hattori, and K. Tanabe, "Catalytic Activities of Binary Metal Oxides Containing Iron for Hydrocracking of Benzyl Phenyl Ether and Diphenyl Ether," *Fuel*, **64**, 1224 (1985).
- McMillen, D. F., and D. M. Golden, "Hydrogen Bond Dissociation Energies," *Ann. Rev. Phys. Chem.*, **33**, 493 (1982).
- Mobley, D. P., and A. T. Bell, "Hydrogenolysis of Dibenzyl Ether Using Zinc Chloride-Metal Cocatalyst Systems," *Fuel*, **57**, 661 (1979).
- Nelder, J. A., and R. Mead, "A Simplex Method for Function Minimization," *Computer J.*, **7**, 308 (1965).
- Penninger, J. M. L. "Reactions of Di-*n*-butylphthalate in Water at Near-critical Temperature and Pressure," *Fuel*, **67**, 490 (1988a).
- , "Chemistry of Methyl-naphthylether in Near-critical Water," *AIChE Meet.* Washington, DC (1988b).
- Press, W. H., B. P. Flannery, S. A. Teukolsky, and W. T. Vetterling, *Numerical Recipes, The Art of Scientific Computing*, Cambridge Univ. Press, Cambridge, (1986).
- Ramayya, S., A. Brittain, C. DeAlmeida, W. Mok, and M. J. Antal, Jr., "Acid-catalyzed Dehydration of Alcohols in Supercritical Waters," *Fuel*, **66**, 1364 (1987).
- Sato, Y., and T. Yamakawa, "Thermal Decomposition of Benzyl Phenyl Ether and Benzyl Phenyl Ketone in the Presence of Tetralin," *Ind. Eng. Chem. Fundam.*, **24**, 12 (1985).
- Schlosberg, R. H., T. R. Ashe, R. Y. Pancirov, and M. Donaldson, "Pyrolysis of Benzyl Ether under Hydrogen Starvation Conditions," *Fuel*, **60**, 155 (1981a).
- Schlosberg, R. H., W. H. Davis, Jr., and T. R. Ashe, "Pyrolysis Studies of Organic Oxygenates. 2: Benzyl Phenyl Ether Pyrolysis under Batch Autoclave Conditions," *Fuel*, **60**, 201 (1981b).
- Schlosberg, R. H., R. F. Szajowski, and G. D. Dupre, "Pyrolysis Studies of Organic Oxygenates. III: High-Temperature Rearrangement of Aryl Alkyl Ethers," *Fuel*, **62**, 690 (1983).
- Simmons, G. M., and D. M. Mason, "Pressure Dependency of Gas Phase Reaction Rate Coefficients," *Chem. Eng. Sci.*, **27**, 89 (1972).
- Stein, S. E., D. A. Robaugh, A. D. Alfieri, and R. E. Miller, "Bond Homolysis in High-Temperature Fluids," *J. Am. Chem. Soc.*, **104**, 6567 (1982).
- Stein, S. R., "A Fundamental Chemical Kinetics Approach to Coal Conversion," *New Approaches in Coal Chemistry, ACS Symp. Ser.*, **169**, 97 (1981).
- Takemura, Y., H. Itoh, and K. Ouchi, "Hydrogenolysis of Coal-Related Model Compounds by Carbon Monoxide-Water Mixture," *Fuel*, **60**, 379 (1981).
- Thies, M. "Vapor-Liquid Equilibrium of Model Coal-Derived Compounds with Methanol at Elevated Temperatures and Pressures," Ph.D. Thesis, Univ. Delaware (1985).
- Townsend, S. H., "Chemical Solvent Effects during Reactions in Supercritical Fluid Solvents," PhD Thesis, Univ. Delaware (1989).
- Townsend, S. H., and M. T. Klein, "Dibenzyl Ether as a Probe into the Supercritical Fluid Solvent Extraction of Volatiles from Coal with Water," *Fuel*, **64**, 635 (1985).
- Townsend, S. H., M. A. Abraham, G. L. Huppert, M. T. Klein, and S. C. Paspek, "Solvent Effects during Reactions in Supercritical Water," *Ind. Eng. Chem. Res.*, **27**, 143 (1988).
- Virk, P. S., "Pericyclic Pathways for 1,2-Diphenylethane Decomposition," *Fuel*, **58**, 149 (1979).
- Wu, B. C., M. T. Klein, and S. I. Sandler, "Reactions in and with Supercritical Fluids: Effect of Phase Behavior on Dibenzyl Ether Pyrolysis Kinetics," *Ind. Eng. Chem. Res.*, **28**, 255 (1989).
- Yang, H. H., and C. A. Eckert, "Homogeneous Catalysis in the Oxidation of *p*-Chlorophenol in Supercritical Water," *Ind. Eng. Chem. Res.*, **27**, 2009 (1988).

Manuscript received Dec. 1, 1989, and revision received May 22, 1990.